TOWARDS BROADBAND OVER POWER LINES SYSTEMS INTEGRATION: TRANSMISSION CHARACTERISTICS OF UNDERGROUND LOW-VOLTAGE DISTRIBUTION POWER LINES

A. G. Lazaropoulos[*]

School of Electrical and Computer Engineering, National Technical University of Athens, 9, Iroon Polytechneiou Street, GR 15780, Zografou Campus, Athens, Greece

Abstract—A complete methodology is employed to determine the transmission characteristics of low-voltage/broadband over power lines (LV/BPL) channels associated with underground power distribution networks, in the light of the multiconductor transmission line (MTL) theory. The established bottom-up approach, already used to treat overhead and underground MV/BPL transmission, is extended to analyze BPL transmission in three-phase N-conductor underground lines with common shield and armor. This analysis shows that these cables may support $N + 2$ modes, giving rise to $N + 2$ separate transmission channels which reduce to $N+1$ if the armor either does not exist or is grounded and to N if the shield is also grounded. In addition to the generalized analysis, a simplified approximation concerning three-phase N-conductor underground cables is also presented. Taking the generalized analysis and the simplified approximation into account, their numerical results concerning attenuation in various underground LV/BPL channels in the frequency range 1–100 MHz are validated against relevant sets of simulations and measurements with satisfactory accuracy and compared to corresponding results of overhead and underground MV/BPL channels. It has been verified that the attenuation in overhead and underground BPL channels depends drastically on power distribution grid type, MTL configuration, and cables used. Moreover, the attenuation in underground LV/BPL channels exhibits a lowpass behavior, is significantly higher than that of overhead MV/BPL ones, and is comparable to that of underground MV/BPL ones. A consequence of the proposed methodology is that it

can facilitate the integration process and intraoperability of LV/BPL and MV/BPL systems through their common physical layer handling.

1. INTRODUCTION

The power distribution grid represents an omnipresent, widely branched hierarchical structure. Therefore, the structure of low-voltage (LV) and medium-voltage (MV) power distribution grids combined with the deployment of broadband over power lines (BPL) networks is the key to developing an advanced IP-based power system, offering both last mile-access and a great number of potential smart grid (SG) applications [1–4].

So far, a plethora of efforts has been made to investigate the broadband potential of LV and MV grids [5–9]. Recently, new interest arises due to the developments regarding multiple-input multiple-output (MIMO) transmission schemes and intraoperability/interoperability of BPL systems [10–13]. The need to harmonize LV/BPL with MV/BPL systems (intraoperability) is a necessary prerequisite before investigating cooperative communications between BPL systems and other broadband technologies (interoperability) [14, 15].

When considered as a transmission medium for communications signals, the LV and MV power grids are subjected to time- and frequency-varying attenuation and exhibit disparity between transmitter/receiver locations due to the network topology, the type of cables, and the connected loads. Also, LV/BPL and MV/BPL networks suffer from various types of noise and must comply with specifications to ensure electromagnetic compatibility (EMC) that limit their available transmitted power [12, 16–19]. The aforementioned adverse factors critically affect the overall performance of BPL channels and the design of BPL systems [6, 20, 21].

An important feature of LV and MV cables is their multiconductor nature. According to multiconductor transmission line (MTL) theory [22, 23], it is known that specific propagating eigenmodes may be defined by various kinds of cables and geometrical arrangements. These eigenmodes correspond to specific distributions of voltages and currents propagating with their own attenuation coefficients and phase delays, independently from each other [24–30].

A hybrid model is usually employed to examine the behavior of BPL transmission channels installed on multiconductor LV and MV lines [25–28]. This model is based on a bottom-up approach to determine the fundamental propagation characteristics (definition of the propagation constant and the characteristic impedance of the modes supported) and on a top-down approach to evaluate the end-

to-end attenuation of a BPL connection. With this hybrid model, it is theoretically possible to compute *a priori* and in a deterministic fashion the end-to-end attenuation of any BPL connection.

In this paper, the bottom-up approach, which has been successfully employed to determine the transmission characteristics of overhead and underground MV/BPL channels [12, 16, 17, 19, 24, 25], is further extended to treat underground LV/BPL transmission in the frequency range 1–100 MHz. The proposed modification of the relevant similarity transformation analysis unifies the BPL analysis for LV/BPL and MV/BPL transmission. LV and MV lines may be treated as three-phase N-conductor underground lines with common shield and armor. In the general case of underground lines, $N + 2$ modes propagate via three-phase N-conductor underground lines with common shield and armor. If the armor is grounded or does not exist, these $N + 2$ modes reduce to $N + 1$ active modes. If the shield is also grounded, these $N + 1$ active modes further reduce to N. The propagation characteristics of these N active modes are derived as a function of the cable geometry and used materials (conductors and dielectric insulations). By applying the extended analysis to underground LV/BPL channels, it is found that the attenuation of underground LV/BPL channels is significantly higher compared to that of overhead MV/BPL channels and comparable to that of underground MV/BPL channels as the behavior of underground LV/BPL channels strongly depends on the type of cables used and the network structure. Moreover, the attenuation in underground LV/BPL channels exhibits a lowpass behavior.

The rest of this paper is organized as follows: In Section 2, the physical BPL layer is examined along with the necessary assumptions concerning LV/BPL and MV/BPL transmission. Section 3 deals with the modal behavior of BPL propagation via three-phase N-conductor underground cables with common shield and armor. The transmission characteristics of BPL propagation are discussed along with the necessary assumptions concerning transmission via the existing real BPL networks. Section 4 presents an approximate solution for underground cables when the dielectric insulation and conductor losses are low. The transmission characteristics of various underground LV/BPL channels are examined via the presented analysis and compared to relevant results of overhead and underground MV/BPL ones. The analytical results are validated against simulations and measurements. Section 5 is devoted to conclusions.

2. THE PHYSICAL BPL LAYER

Signal transmission via power lines differs considerably from signal transmission via the conventional communications mediums (i.e., twisted-pair, coaxial, or fiber-optic cables) due to significant differences in the network topology, grid structure, and the physical properties of power cables [3, 16–18, 20, 25, 28, 31–34].

There is a wide variety of LV and MV distribution power cables. These cables are classified into four major categories [19, 35–37]: 1) the location where the lines are laid. Overhead lines are very common in suburban and rural areas, while their presence in urban areas is diminishing. Underground lines are commonly used in urban areas; 2) the bundling. Single-phase cables have one phase conductor per cable, necessitating three cables per line. Three-phase cables have three phase conductors per cable, necessitating one cable per line; 3) the layout of the cables. It varies according to the number and the type of the conductors (either core- or sector-type, either solid or stranded), the type of insulation, the existence and the number of neutral conductors, the existence of shield and/or armor, the material and the type of the shield and the armor (solid, braided, or taped), and how shielding is accomplished; and 4) the material of the conductors. The most widely used are the aluminium and the copper. Copper is better conductor whereas aluminium is much cheaper.

The proposed analysis is general and considers general case of three-phase N-conductor underground cables with common shield and armor regardless of the type of either the conductors (core- or sector-type) or the insulation. Figure 1 illustrates the layout of this general type of cable. The neutral conductor is a core-type conductor and in galvanic contact with the shield. Thus, the shield is obtained by its concatenation with the neutral conductor.

Signal transmission via three-phase overhead and underground MV power lines has already been analyzed in [16–19, 24–28, 38–46]. This analysis is extended to deal with high-frequency BPL transmission in the general case of underground power lines consisting of three-phase N-conductor with common shield and armor. The following assumptions, which were assumed in the analysis of underground MV power lines, are also made [19, 38, 44, 45]:

A1. N nontwisted solid parallel conductors with common shield and armor and no semiconductor layers are considered, as depicted in Figure 1 [22, 27, 38–40, 43, 47]. The conductors are placed inside a homogeneous insulating medium having permittivity $\varepsilon_{ins}(f)$, permeability μ_0, conductivity σ_{ins}, and dielectric insulation loss
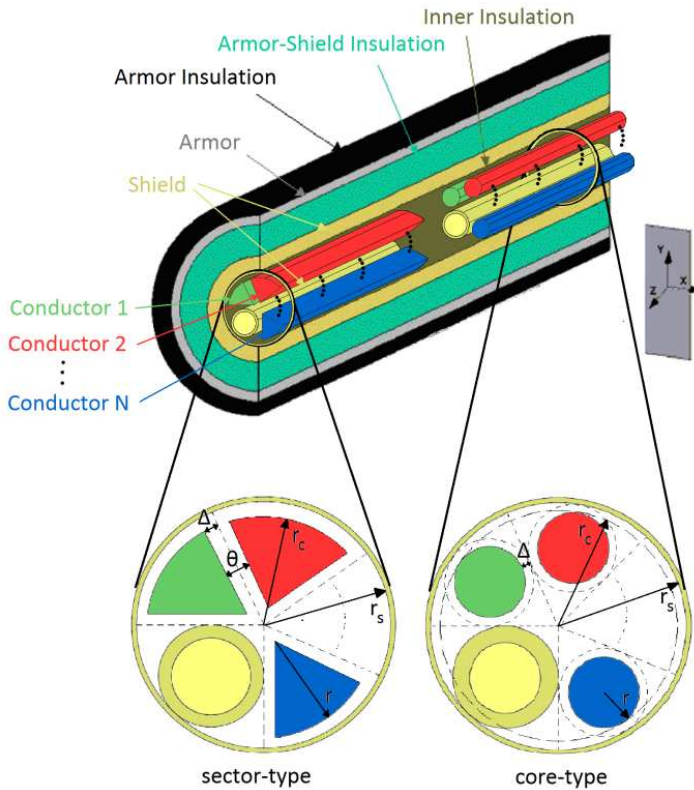
Figure 1. General case of three-phase N-conductor underground cable with common shield and armor [19, 27, 38, 39, 47].

factor $\tan \delta(f)$ [22, 40, 43] where

$$\varepsilon_{ins}(f) = \varepsilon_0 \{\varepsilon_r'(f) - j\varepsilon_r''(f)\} \tag{1}$$

and

$$\tan \delta(f) = \frac{\varepsilon_r''(f)}{\varepsilon_r'(f)} + \frac{\sigma_{ins}}{2\pi f \varepsilon_0 \varepsilon_r'(f)} \approx \frac{\varepsilon_r''(f)}{\varepsilon_r'(f)} \tag{2}$$

In (1) and (2), ε_0 is the free space permittivity, $\varepsilon_r'(f)$ is the relative permittivity of the insulation, and $\varepsilon_r''(f)$ is the imaginary part of its complex relative dielectric constant. Apart from their frequency dependence, $\varepsilon_{ins}(f)$ and $\tan \delta(f)$ depend on the cable type, dielectric insulation material, impregnating mass, age, temperature, mechanical pressure, and various defects (such as water and electrical trees, chemical deterioration, moisture ingress, and air pockets) [20, 27, 40, 48–50].

A2. Since the permittivity and the dielectric insulation loss factor vary from cable to cable, no generic theoretical method exists for their evaluation. Anyway, as usually done to simplify the analysis [19, 22, 24, 27, 40, 43, 49, 51–57], ε_r', ε_r'', and $\tan\delta$ will be assumed constant with regard to frequency. This assumption does not affect the results concerning the transmission characteristics of the examined cables in the range 1–100 MHz when the dielectric insulation losses vary from low — as with cross-linked polyethylene (XLPE) — to very high — as with paper-insulated lead-covered (PILC) cable dielectrics. The assumption is verified by determining the transmission characteristics through appropriately fitting of relevant measurements concerning examined cables in the range 1–100 MHz based on the Debye model [19, 40, 43, 49, 52, 55, 56, 58, 59].

A3. Due to the *quasi*-TEM mode of propagation, the traditional transmission line (TL) theory is appropriate to model BPL signal transmission, either in the overhead or in the underground case [29, 60–63]. A good agreement between BPL models which are based on TL theory and a series of experiments has been validated for frequencies up to 100 MHz [29, 61].

A4. The shield and the armor are considered flawless conductors. The leakage effects due to apertures and imperfections of the conductors are neglected. Since it is reasonable to represent the shield and the armor of cables as solid tubes with annular cross section [20, 24, 27, 38–40, 43–45, 48, 64], the analysis is based on tube impedances first introduced in [47] and [64] for single-phase cables and later extended to multi-phase cables [38, 39, 44, 45, 54, 65].

A5. The influence of the earth return path is negligible due to the electromagnetic shielding provided by the shield and the armor [45, 66]. So the limits of the ground return TL approximation do not affect the analysis of the remaining $N + 1$-conductor TL, namely the N conductors and the shield [38, 45].

A6. The high-frequency behavior of the lossy dielectric insulations is taken into account by the extension of the bottom-up model with the MTL analysis presented in [24, 27, 38, 39, 44, 45, 49, 67–69]. At high frequencies, the relevant losses vary from low to very high. The high-frequency behavior of the cable insulations is incorporated into the relevant analysis by adding to the per-unit-length capacitance element $j2\pi f C_{ij}$ of each per-unit-length admittance matrix element Y_{ij} — referred to in (6) [22, 38, 39, 44], the respective per-unit-length conductance matrix element $G_{ij} = 2\pi f C_{ij}(\tan\delta)_{ij}$ in order to take into account the polarization loss

of the dielectric insulation [20, 40, 48]. C_{ij} and $(\tan \delta)_{ij}$ are the per-unit-length capacitance matrix element of the multi-phase cable and the loss factor of the dielectric insulation surrounding conductors i and j, respectively [22, 24, 27, 38, 45].

Due to the actual structure of the three-phase N-conductor underground LV distribution power lines, the following additional assumption is made [22, 24, 27, 42]:

A7. As it concerns the underground LV power lines, the existence of the armor conductor is not necessary rendering, in these cases, the shield as the outermost conductor [20, 37, 48, 70–73]. Therefore, the high-frequency behavior of the ground is considered into the analysis by incorporating to the per-unit-length impedance and to the per-unit-length admittance of the shield — referred to in (5) and (6), respectively [22, 38, 39, 44] —, the respective ground terms [55, 56, 59, 65]. Moreover, armor terms involved in modal analysis — referred to in Section 3 — are omitted in order not to affect the analysis of the remaining $N + 1$-conductor TL [23, 24, 28, 42, 74–76].

Through a matrix approach, the standard TL analysis can be extended to the MTL case which involves more than two conductors. Compared to a two-conductor line supporting one forward- and one backward-traveling wave, an MTL structure with $n + 1$ conductors parallel to the z axis as depicted in Figure 1 may support n pairs of forward- and backward-traveling waves with corresponding propagation constants. These waves may be described by a coupled set of $2n$ first-order partial differential equations relating the line voltages $V_i(z)$, $i = 1, \ldots, n$ to the line currents $I_i(z)$, $i = 1, \ldots, n$. Each pair of forward- and backward-traveling waves is referred to as a mode [16, 17, 19, 22, 25, 32].

The general cable arrangement consists of the three-phase N conductors (either N sectors or N cores as depicted in Figure 1), one shield conductor and one armor conductor whereas the ground acts as common reference conductor. The line voltages of the conductors, the shield, and the armor are denoted by $V_i(z)$, $i = 1, \ldots, N$, $V_{N+1}(z)$, and $V_{N+2}(z)$, respectively; the respective line currents through the conductors, the shield, and the armor are denoted by $I_i(z)$, $i = 1, \ldots, N$, $I_{N+1}(z)$, and $I_{N+2}(z)$, respectively. The loop voltages $V_i^L(z)$, $i = 1, \ldots, N$ are the voltage differences (vds) between the respective inner conductors and the shield, $V_{N+1}^L(z)$ is the vd between the shield and the armor, and $V_{N+2}^L(z)$ is the vd between the armor and the ground [19, 39, 47]. Based on the above definition of the loop voltages, the associated vector $\mathbf{V}^L(z) =$

$[V_1^L(z) \ldots V_N^L(z) \, V_{N+1}^L(z) \, V_{N+2}^L(z)]^T$ is related to the line voltages vector $\mathbf{V}(z) = [V_1(z) \ldots V_N(z) \, V_{N+1}(z) \, V_{N+2}(z)]^T$ through a simple matrix relationship of the form (see Appendix)

$$\mathbf{V}^L(z) = \mathbf{D}_V^L \mathbf{V}(z) \tag{3}$$

where

$$\mathbf{D}_V^L = \left[\begin{array}{cc|c} \mathbf{I}_N & -1_{N \times 1} & 0_{N \times 1} \\ 0_{1 \times N} & 1 & -1 \\ \hline 0_{1 \times N} & 0 & 1 \end{array} \right] \tag{4}$$

is the loop-to-line vd transformation matrix, $[\cdot]^T$ denotes the transpose of a matrix, $\mathbf{I}_n$ is the $n \times n$ identity matrix, $0_{m \times n}$ is an $m \times n$ matrix with zero elements, and $1_{m \times n}$ is an $m \times n$ matrix with all its elements equal to 1. Likewise, the loop currents $\mathbf{I}^L(z) = [I_1^L(z) \ldots I_N^L(z) \, I_{N+1}^L(z) \, I_{N+2}^L(z)]^T$ can be related to the line currents $\mathbf{I}(z) = [I_1(z) \ldots I_N(z) \, I_{N+1}(z) \, I_{N+2}(z)]^T$ through a similar matrix relationship (see Appendix)

$$\mathbf{I}^L(z) = \mathbf{D}_I^L \mathbf{I}(z) \tag{5}$$

where

$$\mathbf{D}_I^L = \left[\begin{array}{cc|c} \mathbf{I}_N & 0_{N \times 1} & 0_{N \times 1} \\ 1_{1 \times N} & 1 & 0 \\ \hline 1_{1 \times N} & 1 & 1 \end{array} \right] \tag{6}$$

is the loop-to-line current transformation matrix.

The loop voltages and currents are related through the well known coupled differential equations

$$-\frac{d}{dz} \left[\begin{array}{cc} \mathbf{V}^L(z) & \mathbf{I}^L(z) \end{array} \right]^T = \mathrm{diag}\{ \begin{array}{cc} \mathbf{Z} & \mathbf{Y} \end{array} \} \left[\begin{array}{cc} \mathbf{I}^L(z) & \mathbf{V}^L(z) \end{array} \right]^T \tag{7}$$

In (4),

$$\mathbf{Z} = \mathbf{Z}(f) = \left[\begin{array}{cc|c} \mathbf{Z}_{inn}(f) & -\mathbf{Z}_{S-M}(f) & 0_{N \times 1} \\ -\mathbf{Z}_{S-M}^T(f) & Z_{(N+1)(N+1)}(f) & -Z_{A-M}(f) \\ \hline 0_{1 \times N} & -Z_{A-M}(f) & Z_{(N+2)(N+2)}(f) \end{array} \right] \tag{8}$$

is the per-unit-length loop impedance matrix. Equation (8) has been analyzed in [19, 38, 39, 44, 45, 55, 56, 59, 77]. $\mathbf{Z}_{inn}$ is the $N \times N$ per-unit-length impedance matrix of the $N + 1$-conductor TL [22, 24, 27, 40]; $\mathbf{Z}_{S-M}$ is the $N \times 1$ per-unit-length shield-mutual matrix impedance; $Z_{(N+1)(N+1)}$ is the sum of: the per-unit-length shield-out impedance, the insulation between per-unit-length shield-armor impedance, and the per-unit-length armor-in impedance; Z_{A-M} is the per-unit-length armor-mutual impedance; and $Z_{(N+2)(N+2)}$ is the sum of: the

per-unit-length armor-out impedance, the insulation between per-unit-length armor-earth impedance, and the per-unit-length ground impedance [38, 39, 47, 78–80]. $\mathbf{Z}$ is a symmetric matrix [19, 22–28, 81].

The per-unit-length loop admittance matrix $\mathbf{Y}$ appearing in (7) is given by [19, 22, 38, 39, 45, 55, 56, 59], and [82]

$$\mathbf{Y} = \mathbf{Y}(f) = \left[\begin{array}{cc|c} \mathbf{Y}_{inn}(f) & 0_{N\times 1} & 0_{N\times 1} \\ 0_{1\times N} & Y_{(N+1)(N+1)}(f) & -Z_{A-M}(f) \\ \hline 0_{1\times N} & -0 & Y_{(N+2)(N+2)}(f) \end{array} \right] \quad (9)$$

where $\mathbf{Y}_{inn}$ is the $N \times N$ per-unit-length admittance matrix of the aforementioned $N+1$-conductor TL [22, 24, 27, 40, 45, 81]; $Y_{(N+1)(N+1)}$ is the per-unit-length shield-armor insulation admittance; and $Y_{(N+2)(N+2)}$ is the per-unit-length armor earth insulation admittance and the per-unit-length ground admittance in series [38, 39, 47, 78–80, 82]. $\mathbf{Y}$ is a symmetric matrix [19, 22–24, 26–28, 81].

In underground LV/BPL and MV/BPL cables, $\mathbf{Z}$ and $\mathbf{Y}$ relate loop voltages with loop currents, whereas in the overhead MV/BPL case $\mathbf{Z}$ and $\mathbf{Y}$ — as defined in [16, 17, 25, 31–34] — relate line voltages with line currents.

In the case of underground LV/BPL cables with common shield and no armor, under the assumption A7, it is easily shown that the $(N+1) \times (N+1)$ upper left parts of $\mathbf{D}_V^L$, $\mathbf{D}_I^L$, $\mathbf{Z}$, and $\mathbf{Y}$ — as given from (4), (6), (8), and (9), respectively — are the equivalent loop-to-line vd transformation, loop-to-line current transformation, per-unit-length loop impedance matrix, and per-unit-length loop admittance matrices, respectively.

Equations in (7) may be decoupled to yield

$$\frac{d^2}{dz^2} \left[\begin{array}{cc} \mathbf{V}^L(z) & \mathbf{I}^L(z) \end{array} \right]^T = \text{diag}\{ \begin{array}{cc} \mathbf{ZY} & \mathbf{YZ} \end{array} \} \left[\begin{array}{cc} \mathbf{V}^L(z) & \mathbf{I}^L(z) \end{array} \right]^T \quad (10)$$

3. WAVE PROPAGATION VIA THREE-PHASE N-CONDUCTOR UNDERGROUND CABLES WITH COMMON SHIELD AND ARMOR

As in overhead and underground MV/BPL transmission, the modal voltages $\mathbf{V}^m(z) = [V_1^m(z) \ldots V_N^m(z) V_{N+1}^m(z) V_{N+2}^m(z)]^T$ and the modal currents $\mathbf{I}^m(z) = [I_1^m(z) \ldots I_N^m(z) I_{N+1}^m(z) I_{N+2}^m(z)]^T$ may be related to the respective line quantities $\mathbf{V}(z)$ and $\mathbf{I}(z)$ via similarity transformations of the form [16, 17, 19, 22, 83]

$$\left[\begin{array}{cc} \mathbf{V}(z) & \mathbf{I}(z) \end{array} \right]^T = \text{diag}\{ \begin{array}{cc} \mathbf{T}_V & \mathbf{T}_I \end{array} \} \left[\begin{array}{cc} \mathbf{V}^m(z) & \mathbf{I}^m(z) \end{array} \right]^T \quad (11)$$

where $\mathbf{T}_V$ and $\mathbf{T}_I$ are $(N+2) \times (N+2)$ similarity transformation matrices which depend on frequency, the physical properties of the cables,

and the geometry of the MTL configuration [22, 23, 27, 28, 65, 75, 84]. These matrices are determined so that the modal equations, i.e., the differential equations relating the modal quantities, will be decoupled.

The modal equations are derived by substituting (3), (5), (8), (9), and (11) into (10). Then

$$\frac{d^2}{dz^2} [\ \mathbf{V}^m(z) \quad \mathbf{I}^m(z) \ ]^T = \text{diag}\{\ \mathbf{zy} \quad \mathbf{yz} \ \} [\ \mathbf{V}^m(z) \quad \mathbf{I}^m(z) \ ]^T \quad (12)$$

where

$$\mathbf{z} = \mathbf{z}(f) = (\mathbf{D}_V^L \mathbf{T}_V)^{-1} \mathbf{Z} (\mathbf{D}_I^L \mathbf{T}_I) \quad (13)$$

$$\mathbf{y} = \mathbf{y}(f) = (\mathbf{D}_I^L \mathbf{T}_I)^{-1} \mathbf{Y} (\mathbf{D}_V^L \mathbf{T}_V) \quad (14)$$

are the per-unit-length modal impedance $(N+2) \times (N+2)$ matrix and the per-unit-length modal admittance $(N+2) \times (N+2)$ matrix, respectively [16, 17, 19, 22, 26–30, 33, 34, 38, 75, 83].

To determine the various modes that can be supported by the MTL structure, the modal equations in (12) should be decoupled to yield distinct differential equations for each mode. This is accomplished if $\mathbf{T}_V$ and $\mathbf{T}_I$ are determined so that they transform $\mathbf{zy}$ and $\mathbf{yz}$ into diagonal matrices [19, 22–24, 26–28, 81].

Following the same procedure of the underground MV/BPL case [19], in the general underground BPL case, matrices $\mathbf{Z}$ and $\mathbf{Y}$ relate the loop quantities. Consequently, $\mathbf{T}_V$ and $\mathbf{T}_I$ must be determined indirectly. Taking into account (13) and (14), it is readily found that $\mathbf{zy}$ is a diagonal matrix if $\mathbf{D}_V^L \mathbf{T}_V$ is determined so that it diagonalizes the product $\mathbf{ZY}$. Hence, $\mathbf{D}_V^L \mathbf{T}_V$ is the matrix having as its columns the eigenvectors of $\mathbf{ZY}$. Then, $\mathbf{T}_V$, which is employed in the similarity transformations (11), is easily determined. Following the same procedure, $\mathbf{T}_I$ may also be determined [19].

Since $\mathbf{zy}$, $\mathbf{yz}$, $\mathbf{Z}$, and $\mathbf{Y}$ are symmetric matrices and due to (8), (9), (12), (13), and (14), it may easily be shown that $\mathbf{T}_V$ and $\mathbf{T}_I$ are further related through [19, 22–24, 26–28, 81]

$$\left(\mathbf{D}_I^L \mathbf{T}_I\right)^T = \left(\mathbf{D}_V^L \mathbf{T}_V\right)^{-1} \quad (15)$$

Taking into account (13) and (14), the modal voltage of (12) is written as

$$\frac{d^2}{dz^2} \mathbf{V}^m(z) = \lambda \mathbf{V}^m(z) \quad (16)$$

where

$$\lambda = \left(\mathbf{D}_V^L \mathbf{T}_V\right)^{-1} \mathbf{ZY} \left(\mathbf{D}_V^L \mathbf{T}_V\right) = \text{diag}\{\lambda_1 \ \dots \ \lambda_N \ \lambda_{N+1} \ \lambda_{N+2}\} \quad (17)$$

In (17), λ_i, $i = 1, \dots, N+2$, are the eigenvalues of $\mathbf{ZY}$. Then, $\gamma_i = \lambda_i^{1/2} = \alpha_i + j\beta_i$, $i = 1, \dots, N+2$, constitute the propagation

constants of the $N + 2$ modes supported by the underground three-phase N-conductor configuration depicted in Figure 1, namely: (i) $i = 1$ for the common mode (CM) which propagates via the N conductors and returns via the shield. $\gamma_{\mathrm{CM}} \equiv \gamma_1$, $\alpha_{\mathrm{CM}} \equiv \alpha_1$, and $\beta_{\mathrm{CM}} \equiv \beta_1$ constitute the propagation constant, attenuation coefficient, and phase delay of CM, respectively; (ii) $i = 2, \ldots, N$ for the differential modes (DM_{i-1}, $i = 2, \ldots, N$, respectively) which propagate and return via the N conductors. $\gamma_{\mathrm{DM}_{i-1}} \equiv \gamma_i$, $\alpha_{\mathrm{DM}_{i-1}} \equiv \alpha_i$, and $\beta_{\mathrm{DM}_{i-1}} \equiv \beta_i$, $i = 2, \ldots, N$ constitute the propagation constants, attenuation coefficients, and phase delays of DM_{i-1}, $i = 2, \ldots, N$, respectively; and (iii) $i = (N + 1), (N + 2)$ for the phantom modes (PM_1 and PM_2, respectively), one propagating via the shield and returning via the armor and the other propagating via the armor and returning via the earth, respectively. $\gamma_{\mathrm{PM}_{i-N}} \equiv \gamma_i$, $\alpha_{\mathrm{PM}_{i-N}} \equiv \alpha_i$, and $\beta_{\mathrm{PM}_{i-N}} \equiv \beta_i$, $i = (N + 1), (N + 2)$ constitute the propagation constants, attenuation coefficients, and phase delays of PM_{i-N}, $i = (N + 1), (N + 2)$, respectively [16–19, 31–34, 40, 41, 43]. The $N + 2$ modes have their own propagation constants, thus exhibiting different frequency dependence.

Due to (13), (14), and (15), $\mathbf{z}$ and $\mathbf{y}$ are determined from

$$\mathbf{z} = \left(\mathbf{D}_V^L \mathbf{T}_V\right)^{-1} \mathbf{Z} \left(\left(\mathbf{D}_V^L \mathbf{T}_V\right)^T\right)^{-1} = \mathrm{diag}\{z_1 \ \ldots \ z_N \, z_{N+1} \, z_{N+2}\} \quad (18)$$

$$\mathbf{y} = \left(\mathbf{D}_V^L \mathbf{T}_V\right)^T \mathbf{Y} \left(\mathbf{D}_V^L \mathbf{T}_V\right) = \mathrm{diag}\{y_1 \ \ldots \ y_N \, y_{N+1} \, y_{N+2}\} \quad (19)$$

In (18) and (19), z_i, $i = 1, \ldots, N + 2$ and y_i, $i = 1, \ldots, N + 2$ are the per-unit-length modal impedances and the per-unit-length modal admittances of the $N + 2$ modes supported by the MTL configuration, respectively. They constitute the primary cable parameters of the equivalent $N + 2$ modal transmission channels [16, 17, 19, 22, 26–28, 30–34, 38, 75, 83].

Note that the exact solution presented above is a straightforward procedure when the per-unit-length matrices $\mathbf{Z}$ and $\mathbf{Y}$ are exactly known. The expressions derived in the present work concerning BPL transmission are differentiated through the insertion of $\mathbf{D}_V^L$. Similar expressions have been derived in the overhead and the underground MV/BPL case verifying the aforementioned extended analysis [16, 17, 19, 22, 28].

3.1. Transmission Characteristics of Underground BPL Cables in Real Underground Power Distribution Networks

In general, the shield and the armor in three-phase N-conductor underground systems are grounded [36, 37]. Due to the common practice of grounding at both ends, the shield acts as a ground return path and as a reference conductor and separates the N inner

conductors electrostatically and magnetostatically from the remaining set [22, 36, 37]. Hence, the analysis may be focused only on the analysis of the resulting $N + 1$-conductor TL. This separation is the common procedure either in theoretical analyses or in measurements [23, 27, 38–40, 42, 43, 48, 74–76, 82, 85, 86]. As the phantom modes are not practically involved in BPL transmission, their spectral behavior will not be considered further. This has also been observed in underground MV/BPL transmission [19].

4. APPROXIMATE SOLUTION FOR UNDERGROUND BPL CABLES WITH LOW DIELECTRIC INSULATION AND MODAL CONDUCTOR LOSSES

In this Section, the SART approximation is applied — named after the author first proposed it in [24, 26, 27] — concerning three-phase N-conductor underground cables with at both ends grounded common shield regardless of the armor existence and the conductor type (either core- or sector-type). This approximation aims at approximately solving the remaining $N + 1$-conductor TL eigenproblem for three-phase N-conductor underground cables with low dielectric insulation losses $\tan \delta(f)$ and modal conductor losses $\delta_{c_i}(f)$, $i = 1, \ldots, N$ where

$$\delta_{c_i}(f) = \frac{\text{Re}\{z_i\}}{\text{Im}\{z_i\}} = \frac{\delta_{c_i}^0(f)}{\sqrt{f}}, \quad i = 1, \ldots, N \tag{20}$$

are the conductor losses for the N modes supported by the $N + 1$-conductor TL. In (20), $\delta_{c_i}^0(f)$, $i = 1, \ldots, N$ are the modal conductor loss angles and are assumed constant for each mode with regard to frequency, as usually done to simplify the analysis [24, 26, 27, 56]. $\delta_{c_i}(f)$, $i = 1, \ldots, N$ and $\delta_{c_i}^0(f)$, $i = 1, \ldots, N$ depend on skin effect, temperature, current, type and material of the conductors, type and material of the shield, and cable geometry [20, 24, 26, 27, 48, 50–53, 74]. It should be noted the SART approximation is valid for the vast majority of cables employed in existing underground LV distribution power grids [35, 50, 51, 70–72].

For these types of cables, it turns out that, when the losses are low, namely $\tan \delta \ll 1$ and $\delta_{c_i}(f) \ll 1$, $i = 1, \ldots, N$, the attenuation coefficients α_i, $i = 1, \ldots, N$ and phase delays β_i, $i = 1, \ldots, N$ of the N modes supported by the $N + 1$-conductor TL are given by [24, 26, 27, 48, 73]

$$\alpha_i \approx \frac{\pi f \sqrt{\varepsilon_r'}}{c} [\tan \delta + \delta_{c_i}(f)], \quad i = 1, \ldots, N \tag{21}$$

$$\beta_i \approx \frac{\pi f \sqrt{\varepsilon_r'}}{c} [2 + \delta_{c_i}(f)], \quad i = 1, \ldots, N \tag{22}$$

From (21) and (22), it is deduced that the attenuation coefficients and the phase delays exhibit an increasing behavior with respect to frequency. Apart from their dependence on frequency, the transmission characteristics depend on the specific configuration of the $N + 1$-conductor TL and the material parameters.

Although the theoretical analysis presented in Section 3 is general and considers three-phase N-conductor underground cables with common shield and armor regardless of the conductor type and the insulation, the underground LV/BPL cables that will be examined in the simulation consist of representative LV cables used in underground LV power distribution networks. Hence, various three-phase three- or four-conductor underground LV/BPL cables with common shield and no armor are considered, as depicted in Figures 2(a)–(e) [35, 50, 51, 70, 71].

In Figures 3(a) and 3(b), the attenuation coefficients α_{CM} and $\alpha_{DM_{i-1}}$, $i = 2, \ldots, N$ of the underground LV configurations presented in Figures 2(a) and 2(b), respectively, are plotted versus frequency, whereas the phase delays β_{CM} and $\beta_{DM_{i-1}}$, $i = 2, \ldots, N$ behave similar to attenuation coefficients and are not plotted — this has also
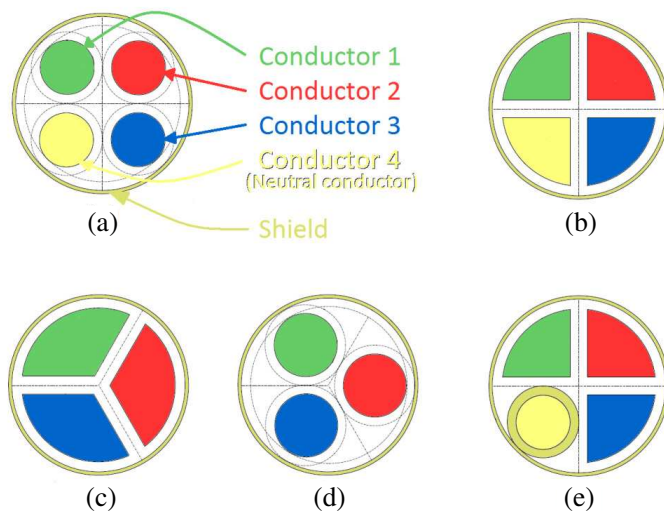

Figure 2. Main categories of three-phase underground LV distribution cables with common shield and no armor [27, 38, 39, 47]. (a) Four-conductor core-type cable. (b) Four-conductor sector-type cable. (c) Three-conductor sector-type cable. (d) Three-conductor core-type cable. (e) Three-conductor cable with the shield concatenated with the core-type neutral conductor.

been observed in underground MV/BPL transmission [19, 40, 41, 43] —. More analytically, as observed from Figures 3(a) and 3(b), the aforementioned theoretical analysis is validated by using:

- the simulation results, as presented in [87], concerning: (i) the three-phase four-conductor core-type YJV underground LV distribution cable ($4 \times 25 \, mm^2$ Cu, XLPE) as depicted in Figure 2(a) — see Figure 3(a) —; and (ii) the three-phase four-conductor sector-type YJLV underground LV distribution cable ($4 \times 95 \, mm^2$ Al, XLPE) as depicted in Figure 2(b) — see Figure 3(b) —;
- the extended underground MTL transmission analysis — see Figure 3(a) — concerning the aforementioned three-phase four-
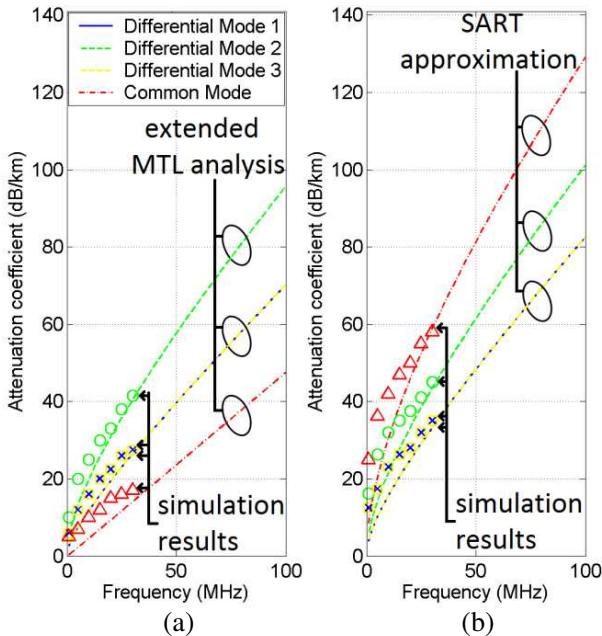

Figure 3. Attenuation coefficients of underground LV/BPL cables (linear scale is used for the y-axes and the legend is common for both plots). (a) Simulation results concerning the three-phase four-conductor core-type YJV underground LV distribution cable are compared with the extended underground MTL transmission analysis. (b) Simulation results concerning the three-phase four-conductor sector-type YJLV underground LV distribution cable are compared with the SART approximation.

conductor core-type YJV underground LV distribution cable buried 1 m inside the ground. The conductivity of the ground is assumed $\sigma_g = 5\,\text{mS/m}$ and its relative permittivity $\varepsilon_{rg} = 13$ which is a realistic scenario [16–18, 25, 31–34].

- the SART approximation — see Figure 3(b) — concerning the aforementioned three-phase four-conductor sector-type YJLV underground LV distribution cable.

Due to its simplicity and generality, the SART approximation will be adopted for the rest of the simulations.

Several deterministic, stochastic, and statistical models concerning the evaluation of LV/BPL channels have been proposed [1, 24–28, 38, 45, 46, 54–59, 88, 89]. Over the recent years, various measurements concerning the underground LV distribution grid for various topologies and cables types have been performed in the frequency range from 1–30 MHz and 1–100 MHz. These measurements may be classified into the following sets:

- field trial measurements in real underground LV/BPL networks, including: 1) OPERA [35, 88]; 2) GERman LV power grid [20, 48, 73]; and 3) INDian LV power grid [89];
- experimental measurements of LV cables, including the: 1) EDF (HN33S33, $3\times150+70\,\text{mm}^2$ Al, PVC, Steel-Pb shield) — depicted in Figure 2(e) — denoted as EDF/CM and EDF/DM$_1$ for CM and DM$_1$, respectively [24, 27, 46]; 2) DOS (NYCY, $3 \times 70\,\text{mm}^2$ Cu, PVC) — depicted in Figure 2(c) — [48, 72]; and 3) ARI (NYM, $3 \times 2.5\,\text{mm}^2$ Cu, PVC) — depicted in Figure 2(d) — [56, 72].

The above sets of measurements and the attenuation coefficients α_{CM}, α_{DM_1}, and α_{DM_2} of the aforementioned HN33S33 underground LV/BPL cable — denoted as underground LV — are plotted versus frequency in Figure 4. Moreover, the attenuation coefficients concerning MV/BPL transmission via specific MV/BPL cable configurations are also plotted, being classified into the following set:

- simulation results of MV/BPL networks, including: 1) overhead MV grid — denoted as overhead MV and presented analytically in [16–18, 31–34] —; and 2) underground MV grid where shielded PILC cables are used — denoted as underground MV and presented analytically in [12, 19, 40, 43] —.

As readily observed from Figure 4, the validity of the proposed theoretical analysis — underground LV curves — is also verified by experimental measurements — EDF/CM and EDF/DM$_1$ markers —. The slight divergence existing between the two sets of results is attributed to various kinds of line apertures, imperfections, and other

inhomogeneities of the geometrical and electrical characteristics of the cable under test and the experimental setup used [24, 27, 46]. It is also confirmed that the HN33S33 underground LV/BPL cable behaves relatively close to the line-of-sight ("LOS") transmission behavior (corresponding to "LOS" transmission in wireless channels) of the majority of existing real underground LV distribution power grids and, hence, may provide a representative picture of the real world situation.

As for the spectral behavior of underground LV/BPL channels, the following general conclusions are deduced:
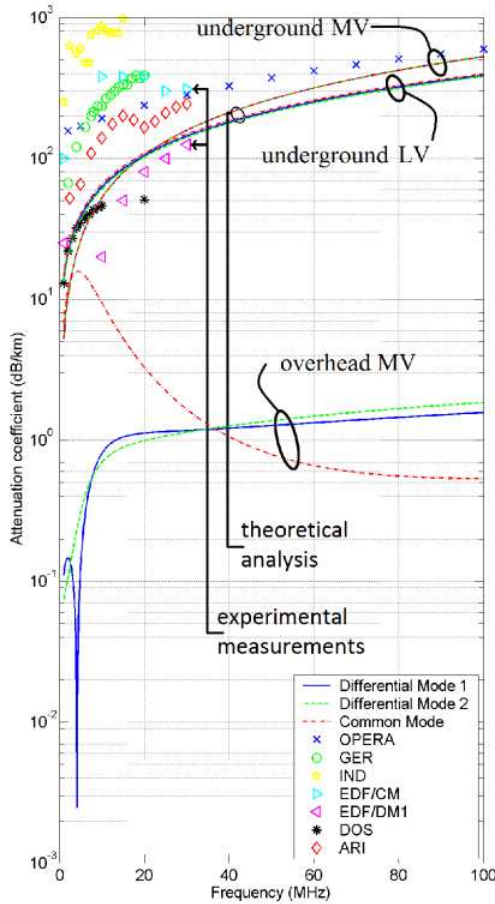

Figure 4. Attenuation of overhead and underground BPL channels plotted versus frequency (subchannel frequency span is equal to 0.1 MHz and logarithmic scale is used for the *y*-axis).

- Apart from its frequency dependence, broadband transmission via underground LV/BPL networks depends drastically on the cable parameters, underground LV grid topology, national wiring and grounding practices, MV/LV transformer crosstalk, issues related to asymmetries of the line and the LV configuration parameters, coupling, leakage currents, and other imperfections [1, 18, 29, 30, 35, 45, 83, 88].

- Attenuation in underground LV/BPL transmission channels is higher than that of overhead MV/BPL ones whereas is comparable to that of underground MV/BPL ones [35, 88].

- The end-to-end attenuation of the underground LV/BPL power distribution networks is an increasing function of frequency exhibiting lowpass spectral behavior characteristics [19, 20, 24, 27, 46, 48, 72].

As for the spectral behavior of the N active modes of underground LV/BPL distribution cables with low dielectric insulation and modal conductor losses, the following additional conclusions are deduced:

- Unlike underground MV/BPL channels — where the three active modes CM, DM_1 and DM_2 exhibit an almost identical spectral behavior — and overhead MV/BPL channels — where DM_1 and DM_2 behave almost identically whereas the behavior of the CM is quite different — in underground LV/BPL power distribution channels, the N active modes — CM and DM_{i-1}, $i = 2, \ldots, N$ — exhibit different behaviors depending primarily on the cable configuration and material parameters. The primary high-frequency loss mechanisms are the mode-dependent conductor losses — caused by the proximity effect (skin effect) — and the dielectric insulation losses [1, 18, 19, 22–30, 35, 36, 40, 43, 45, 46, 48–51, 83, 88, 90].

- The concept of multiconductor diversity permits a boost of the overall channel capacity (MIMO/BPL technology) by appropriately exploiting the conductors of the MTL configurations and by simultaneously complying with specifications to ensure EMC. The significant increase in data throughput, link reliability, diversity, and range without additional bandwidth or transmit power permits a wide variety of BPL technologies finding a role in most key SG applications [10–12, 14, 18, 27].

Concluding the above BPL technology analysis, it should be highlighted that SG will be supported by a heterogeneous set of networking technologies, as no single solution fits all scenarios. LV/BPL and MV/BPL systems need to work in a compatible way (intraoperate) before BPL technology interoperates with other

broadband technologies, such as wired (e.g., fiber and DSL) and wireless (e.g., WiFi and WiMax). Compatible frequencies, equipment and signaling, adequate injected power spectral density (IPSD) levels, area coverage, and scalable capacity must be ensured, taking the specific features of LV/BPL and MV/BPL transmission into account [1, 2, 12–19].

5. DISCUSSION AND CONCLUSIONS

The transmission characteristics of three-phase underground LV/BPL channels have been studied and compared to those of three-phase overhead and underground MV/BPL ones. By properly combining the similarity transformation with MTL theory, the modal differential equations are decoupled, giving rise to $N + 2$ separate propagating modes. If the armor is grounded or does not exist, these $N + 2$ modes reduce to $N+1$ active modes. If the shield is also grounded, these $N+1$ active modes further reduce to N which, as shown by the numerical results, exhibit different behaviors. The numerical results show that underground LV/BPL transmission exhibits a lowpass behavior and the attenuation of underground LV/BPL power distribution channels is higher compared to that of overhead MV/BPL ones and comparable to that of underground MV/BPL ones in the frequency range 1–100 MHz.

APPENDIX A. LOOP VOLTAGES AND CURRENTS

Extending the analysis presented in [19], based on their definition, V_i^L, $i = 1, \ldots, N+2$ and V_i, $i = 1, \ldots, N+2$, are related through [38, 39, 47]

$$V_i^L = V_i - V_{N+1}\, i = 1, \ldots, N,\ V_{N+1}^L = V_{N+1} - V_{N+2},\ V_{N+2}^L = V_{N+2} \quad \text{(A1)}$$

wherefrom $\mathbf{D}_V^L$ may easily be evaluated to yield (4).

Also, the loop currents I_i^L, $i = 1, \ldots, N + 2$ are related to the line currents I_i, $i = 1, \ldots, N + 2$ through [38, 39, 45]

$$I_i^L = I_i\, i = 1, \ldots, N,\ I_{N+1}^L = \sum_{i=1}^{N+1} I_i,\ I_{N+2}^L = \sum_{i=1}^{N+2} I_i \qquad \text{(A2)}$$

From (A2), $\mathbf{D}_I^L$ may easily be evaluated yielding (6).

REFERENCES

1. Galli, S., "A novel approach to the statistical modeling of wireline channels," *IEEE Trans. Commun.*, Vol. 59, No. 5, 1332–1345, May 2011.

2. Galli, S., A. Scaglione, and Z. Wang, "For the grid and through the grid: The role of power line communications in the smart grid," *Proc. IEEE*, Vol. 99, No. 6, 998–1027, Jun. 2011.

3. Gebhardt, M., F. Weinmann, and K. Dostert, "Physical and regulatory constraints for communication over the power supply grid," *IEEE Commun. Mag.*, Vol. 41, No. 5, 84–90, May 2003.

4. Jee, G., C. Edison, R. Das Rao, and Y. Cern, "Demonstration of the technical viability of PLC systems on medium- and low-voltage lines in the United States," *IEEE Commun. Mag.*, Vol. 41, No. 5, 108–112, May 2003.

5. Galli, S., A. Scaglione, and K. Dostert, "Broadband is power: Internet access through the power line network," *IEEE Commun. Mag.*, Vol. 41, No. 5, 82–83, May 2003.

6. Götz, M., M. Rapp, and K. Dostert, "Power line channel characteristics and their effect on communication system design," *IEEE Commun. Mag.*, Vol. 42, No. 4, 78–86, Apr. 2004.

7. Amirshahi, P. and M. Kavehrad, "Medium voltage overhead power-line broadband communications; transmission capacity and electromagnetic interference," *Proc. IEEE Int. Symp. Power Line Communications Applications*, 2–6, Vancouver, BC, Canada, Apr. 2005.

8. Aquilué, R., M. Ribó, J. R. Regué, J. L. Pijoan, and G. Sánchez, "Scattering parameters-based channel characterization and modeling for underground medium-voltage power-line communications," *IEEE Trans. Power Del.*, Vol. 24, No. 3, 1122–1131, Jul. 2009.

9. Tonello, A. M., F. Versolatto, and S. D'Alessandro, "Opportunistic relaying in in-home PLC networks," *Proc. IEEE Global Telecommunications Conference*, 1–5, Miami, FL, USA, Dec. 2010.

10. Versolatto, F. and A. M. Tonello, "An MTL theory approach for the simulation of MIMO power-line communication channels," *IEEE Trans. Power Del.*, Vol. 26, No. 3, 1710–1717, Jul. 2011.

11. Schneider, D., J. Speidel, L. Stadelmeier, and D. Schill, "Precoded spatial multiplexing MIMO for inhome power line communications," *Proc. IEEE Global Telecommunications Conference*, 1–5, New Orleans, LA, USA, Nov./Dec. 2008.

12. Lazaropoulos, A. G. and P. G. Cottis, "Broadband transmission via underground medium-voltage power lines — Part II: Capacity," *IEEE Trans. Power Del.*, Vol. 25, No. 4, 2425–2434, Oct. 2010.

13. Oksman, V. and S. Galli, "G.hn: The new ITU-T home networking standard," *IEEE Commun. Mag.*, Vol. 47, No. 10, 138–145, Oct. 2009.

14. OPERA2, D51: White Paper: OPERA technology (final version). IST Integrated Project, No. 026920, Dec. 2008.

15. Kuhn, M., S. Berger, I. Hammerström, and A. Wittneben, "Power line enhanced cooperative wireless communications," *IEEE J. Sel. Areas Commun.*, Vol. 24, No. 7, 1401–1410, Jul. 2006.

16. Lazaropoulos, A. G., "Broadband transmission characteristics of overhead high-voltage power line communication channels," *Progress In Electromagnetics Research B*, Vol. 36, 373–398, 2012.

17. Lazaropoulos, A. G. and P. G. Cottis, "Transmission characteristics of overhead medium voltage power line communication channels," *IEEE Trans. Power Del.*, Vol. 24, No. 3, 1164–1173, Jul. 2009.

18. Lazaropoulos, A. G. and P. G. Cottis, "Capacity of overhead medium voltage power line communication channels," *IEEE Trans. Power Del.*, Vol. 25, No. 2, 723–733, Apr. 2010.

19. Lazaropoulos, A. G. and P. G. Cottis, "Broadband transmission via underground medium-voltage power lines — Part I: Transmission characteristics," *IEEE Trans. Power Del.*, Vol. 25, No. 4, 2414–2424, Oct. 2010.

20. Zimmermann, M. and K. Dostert, "A multipath model for the powerline channel," *IEEE Trans. Commun.*, Vol. 50, No. 4, 553–559, Apr. 2002.

21. Galli, S. and O. Logvinov, "Recent developments in the standardization of power line communications within the IEEE," *IEEE Commun. Mag.*, Vol. 46, No. 7, 64–71, Jul. 2008.

22. Paul, C. R., *Analysis of Multiconductor Transmission Lines*, Wiley, New York, 1994.

23. Faria, J. A. B., *Multiconductor Transmission-Line Structures: Modal Analysis Techniques*, Wiley, New York, 1994.

24. Sartenaer, T. and P. Delogne, "Deterministic modelling of the (shielded) outdoor powerline channel based on the multiconductor transmission line equations," *IEEE J. Sel. Areas Commun.*, Vol. 24, No. 7, 1277–1291, Jul. 2006.

25. Amirshahi, P. and M. Kavehrad, "High-frequency characteristics of overhead multiconductor power lines for broadband communications," *IEEE J. Sel. Areas Commun.*, Vol. 24, No. 7, 1292–1303, Jul. 2006.

26. Sartenaer, T. and P. Delogne, "Powerline cables modelling for

broadband communications," *Proc. IEEE Int. Conf. Power Line Communications and Its Applications*, 331–337, Malmö, Sweden, Apr. 2001.

27. Sartenaer, T., "Multiuser communications over frequency selective wired channels and applications to the powerline access network," Ph.D. Dissertation, Univ. Catholique Louvain, Louvain-la-Neuve, Belgium, Sep. 2004. [Online]. Available: http://www.tele.ucl.ac.be/∼ts/PhD.php.

28. Calliacoudas, T. and F. Issa, ""Multiconductor transmission lines and cables solver," an efficient simulation tool for plc channel networks development," *IEEE Int. Conf. Power Line Communications and Its Applications*, Athens, Greece, Mar. 2002.

29. Galli, S. and T. Banwell, "A deterministic frequency-domain model for the indoor power line transfer function," *IEEE J. Sel. Areas Commun.*, Vol. 24, No. 7, 1304–1316, Jul. 2006.

30. Pérez, A., A. M. Sánchez, J. R. Regué, M. Ribó, R. Aquilué, P. Rodríguez-Cepeda, and F. J. Pajares, "Circuital and modal characterization of the power-line network in the PLC band," *IEEE Trans. Power Del.*, Vol. 24, No. 3, 1182–1189, Jul. 2009.

31. D'Amore, M. and M. S. Sarto, "A new formulation of lossy ground return parameters for transient analysis of multiconductor dissipative lines," *IEEE Trans. Power Del.*, Vol. 12, No. 1, 303–314, Jan. 1997.

32. Amirshahi, P., "Broadband access and home networking through powerline networks," Ph.D. Dissertation, Pennsylvania State Univ., University Park, PA, May 2006. [Online]. Available: http://etda.libraries.psu.edu/theses/approved/WorldWideIndex-/ETD-1205/index.html.

33. D'Amore, M. and M. S. Sarto, "Simulation models of a dissipative transmission line above a lossy ground for a wide-frequency range — Part I: Single conductor configuration," *IEEE Trans. Electromagn. Compat.*, Vol. 38, No. 2, 127–138, May 1996.

34. D'Amore, M. and M. S. Sarto, "Simulation models of a dissipative transmission line above a lossy ground for a wide-frequency range — Part II: Multi-conductor configuration," *IEEE Trans. Electromagn. Compat.*, Vol. 38, No. 2, 139–149, May 1996.

35. OPERA1, D44: Report presenting the architecture of plc system, the electricity network topologies, the operating modes and the equipment over which PLC access system will be installed, IST Integr. Project No. 507667, Dec. 2005. [Online]. Available: http://www.ist-opera.org/opera1/downloads/D44_Architecture_PLC.zip.

36. US Department of Defence, Military Handbook. Grounding, Bonding, and Shielding for Electronic Equipments and Facilities. Vol. 1: Basic Theory Washington, DC, Tech. Rep., ADA239565, Dec. 1987. [Online]. Available: http://www.wbdg.org/ccb/FEDMIL/hdbk419_vol1.pdf.

37. Stallcup, J. G., *Stallcup's Electrical Grounding and Bonding Simplified*, 2005 Edition, Jones & Bartlett, Boston, MA, 2005.

38. Theethayi, N., "Electromagnetic interference in distributed outdoor electrical systems, with an emphasis on lightning interaction with electrified railway network," Ph.D. Dissertation, Uppsala Univ., Uppsala, Sweden, Sep. 2005. [Online]. Available: http://uu.diva-portal.org/smash/get/diva2:166746/FULLTEXT01.

39. Theethayi, N., Z. Mazloom, and R. Thottappillil, "Technique for reducing transient voltages in multiconductor-shielded cables," *IEEE Trans. Electromagn. Compat.*, Vol. 49, No. 2, 434–440, May 2007.

40. Van der Wielen, P. C. J. M., "On-line detection and location of partial discharges in medium-voltage power cables," Ph.D. Dissertation, Tech. Univ. Eindhoven, Eindhoven, the Netherlands, Apr. 2005. [Online]. Available: http://alexandria.tue.nl/extra2/200511097.pdf.

41. Van der Wielen, P. C. J. M., E. F. Steennis, and P. A. A. F. Wouters, "Fundamental aspects of excitation and propagation of on-line partial discharge signals in three-phase medium voltage cable systems," *IEEE Trans. Dielectr. Electr. Insul.*, Vol. 10, No. 4, 678–688, Aug. 2003.

42. Ofcom, Compatibility of VDSL & PLT with radio services in the range 1.6 MHz to 30 MHz Ofcom, Oct. 2002. [Online]. Available: http://www.ofcom.org.uk/static/archive/ra/topics/interference-/documents/twg-finalreport.pdf.

43. Veen, J., "On-line signal analysis of partial discharges in medium voltage power cables," Ph.D. Dissertation, Tech. Univ. Eindhoven, Eindhoven, the Netherlands, Apr. 2005. [Online]. Available: http://alexandria.tue.nl/extra2/200511099.pdf.

44. Theethayi, N., R. Thottappillil, M. Paolone, C. A. Nucci, and F. Rachidi, "External impedance and admittance of buried horizontal wires for transient studies using transmission line analysis," *IEEE Trans. Dielectr. Electr. Insul.*, Vol. 14, No. 3, 751–761, Jun. 2007.

45. Rachidi, F. and S. V. Tkachenko, *Electromagnetic Field Interaction with Transmission Lines: From Classical Theory to*

HF Radiation Effects, WIT Press, Southampton, UK, 2008.

46. Issa, F., D. Chaffanjon, E. P. de la Bâthie, and A. Pacaud, "An efficient tool for modal analysis transmission lines for PLC networks development," *IEEE Int. Conf. Power Line Communications and Its Applications*, Athens, Greece, Mar. 2002.

47. Wedepohl, L. M. and D. J. Wilcox, "Transient analysis of underground power transmission systems. System-model and wave propagation characteristics," *Proc. Inst. Elect. Eng.*, Vol. 120, No. 2, 253–260, Feb. 1973.

48. Dostert, K., *Powerline Communications*, Prentice-Hall, Upper Saddle River, NJ, 2001.

49. Mugala, G., "High frequency characteristics of medium voltage XLPE power cables," Ph.D. Dissertation, KTH Royal Inst. Technol., Stockholm, Sweden, Nov. 2005. [Online]. Available: http://kth.diva-portal.org/smash/get/diva2:14437/FULLTEXT01.

50. Clark, F. M., *Insulating Materials for Design and Engineering Practice*, Wiley, New York, 1962.

51. Xu, C., L. Zhou, J. Y. Zhou, and S. Boggs, "High frequency properties of shielded power cable — Part 1: Overview of mechanism," *IEEE Electr. Insul. Mag.*, Vol. 21, No. 6, 24–28, Nov./Dec. 2005.

52. Gustavsen, B., J. A. Martinez, and D. Durbak, "Parameter determination for modeling system transients — Part II: Insulated cables," *IEEE Trans. Power Del.*, Vol. 20, No. 3, 2045–2050, Jul. 2005.

53. Galanis, L. K., H. T. Anastassiu, and S. A. Kotsopoulos, "Wide band, accurate estimation for the primary parameters of the NA2XCWY underground cable," *Proc. IEEE Int. Symp. Power Line Communications and Its Applications*, 314–318, Pisa, Italy, Mar. 2007.

54. Grassi, F. and S. A. Pignari, "Data-transmission characteristics of power cables with star-quad cross-section," *Proc. IEEE Int. Symp. Power Line Communications and Its Applications*, 401–406, Pisa, Italy, Mar. 2007.

55. Andreou, G. T. and D. P. Labridis, "Electrical parameters of low-voltage power distribution cables used for power-line communications," *IEEE Trans. Power Del.*, Vol. 22, No. 2, 879–886, Apr. 2007.

56. Andreou, G. T., E. K. Manitsas, D. P. Labridis, P. L. Katsis, F. N. Pavlidou, and P. S. Dokopoulos, "Finite element

characterization of LV power distribution lines for high frequency communication signals," *Proc. IEEE Int. Symp. Power Line Communications and Its Applications*, 109–113, Kyoto, Japan, Mar. 2003.

57. Dickinson, J. and P. Nicholson, "Calculating the high frequency transmission line parameters of power cables," *Proc. IEEE Int. Symp. Power Line Communications and Its Applications*, 127–133, Essen, Germany, Apr. 1997.

58. Breien, O. and I. Johansen, "Attenuation of traveling waves in single-phase high-voltage cables," *Proc. Inst. Elect. Eng.*, Vol. 118, 787–793, Jun. 1971.

59. Andreou, G. T. and D. P. Labridis, "Experimental evaluation of a low-voltage power distribution cable model based on a finite-element approach," *IEEE Trans. Power Del.*, Vol. 22, No. 3, 1455–1460, Jul. 2007.

60. Anatory, J. and N. Theethayi, "On the efficacy of using ground return in the broadband power-line communications-A transmission-line analysis," *IEEE Trans. Power Del.*, Vol. 23, No. 1, 132–139, Jan. 2008.

61. Anatory, J., N. Theethayi, R. Thottappillil, M. M. Kissaka, and N. H. Mvungi, "An experimental validation for broadband power-line communication (BPLC) model," *IEEE Trans. Power Del.*, Vol. 23, No. 3, 1380–1383, Jul. 2008.

62. Galli, S., "Exact conditions for the symmetry of a loop," *IEEE Commun. Lett.*, Vol. 4, No. 10, 307–309, Oct. 2000.

63. Banwell, T. and S. Galli, "A new approach to the modeling of the transfer function of the power line channel," *Proc. IEEE Int. Symp. Power Line Communications and Its Applications*, 319–324, Malmö, Sweden, Apr. 2001.

64. Schelkunoff, S. A., *Electromagnetic Waves*, Van Nostrand, Princeton, NJ, 1943.

65. Papagiannis, G. and P. Dokopoulos, "A simplified real frequency independent modal transformation for overhead line switching transient computations," *Europ. Trans. on Electrical Power*, Vol. 5, No. 5, 307–314, Sep./Oct. 1995.

66. Wedepohl, L. M., "Application of the solution of traveling-wave phenomena in polyphase system," *Proc. Inst. Elect. Eng.*, Vol. 110, No. 12, 2200–2212, Dec. 1963.

67. Mugala, G., R. Eriksson, U. Gafvert, and P. Pettersson, "Measurement technique for high frequency characterization of semiconducting materials in extruded cables," *IEEE Trans.*

Dielectr. Electr. Insul., Vol. 11, No. 3, 471–480, Jun. 2004.

68. Mugala, G., R. Eriksson, and P. Pettersson, "Dependence of XLPE insulated power cable wave propagation characteristics on design parameters," *IEEE Trans. Dielectr. Electr. Insul.*, Vol. 14, No. 2, 393–399, Apr. 2007.

69. Mugala, G., R. Eriksson, and P. Pettersson, "Comparing two measurement techniques for high frequency characterization of power cable semiconducting and insulating materials," *IEEE Trans. Dielectr. Electr. Insul.*, Vol. 13, No. 4, 712–716, Aug. 2006.

70. Nexans Deutschland Industries GmbH & Co. KG-catalogue LV underground power cables distribution cables, Feb. 2011.

71. Elkabel Bulgaria-catalogue cables and wires, Feb. 2010. [Online]. Available: http://www-en.elma-bg.com/files/Elkabel_en.pdf.

72. Tele-Fonika Kable GmbH, Cables and wires, 2008. [Online]. Available: http://www.jauda.com/upload_file/Katalogi/citi-/Telefonika/tfb2008.pdf.

73. Zimmermann, M. and K. Dostert, "A multi-path signal propagation model for the power line channel in the high frequency range," *Proc. IEEE Int. Symp. Power Line Communications and Its Applications*, 45–51, Lancaster, UK, Mar. 1999.

74. Brown, P. A., "Evaluation of the screening efficiency at HF of low voltage electricity distribution cables with a concentric metallic sheath by the application of surface transfer impedance methods," *IEEE Int. Conf. Power Line Communications and Its Applications*, Athens, Greece, Mar. 2002.

75. Faria, J. A. B., "Application of Clarke's transformation to the modal analysis of asymmetrical single-circuit three-phase line configurations," *Europ. Trans. on Electrical Power*, Vol. 10, No. 4, 225–231, Jul./Aug. 2000.

76. Meng, H., S. Chen, Y. L. Guan, C. L. Law, P. L. So, E. Gunawan, and T. T. Lie, "Modeling of transfer characteristics for the broadband power line communication channel," *IEEE Trans. Power Del.*, Vol. 19, No. 3, 1057–1064, Jul. 2004.

77. Theethayi, N., Y. Baba, F. Rachidi, and R. Thottappillil, "On the choice between transmission line equations and full-wave Maxwell's equations for transient analysis of buried wires," *IEEE Trans. Electromagn. Compat.*, Vol. 50, No. 2, 347–357, May 2008.

78. Schelkunoff, S. A., "The electromagnetic theory of coaxial transmission lines and cylindrical shields," *J. Bell Syst. Tech.*, Vol. 13, 532–579, Oct. 1934.

79. Pollaczek, F., "Über das feld einer unendlich langenwechsel

stromdurchflossenen einfachleitung," *Elek. Nachr. Tech.*, Vol. 3, No. 9, 339–360, 1926.

80. Sunde, E. D., *Earth Conduction Effects in the Transmission Systems*, Van Nostrand, New York, 1949.

81. Davis, P. J., *Circulant Matrices*, Wiley, New York, 1979.

82. Vance, E. F., *Coupling to Cable Shields*, Wiley, New York, 1978.

83. Banwell, T. and S. Galli, "A novel approach to accurate modeling of the indoor power line channel — Part I: Circuit analysis and companion model," *IEEE Trans. Power Del.*, Vol. 20, No. 2, Part 1, 655–663, Apr. 2005.

84. Anatory, J., N. Theethayi, and R. Thottappillil, "Power-line communication channel model for interconnected networks — Part II: Multiconductor system," *IEEE Trans. Power Del.*, Vol. 24, No. 1, 124–128, Jan. 2009.

85. Aquilué, R., "Power line communications for the electrical utility: Physical layer design and channel modeling," Ph.D. Dissertation, Univ. Ramon Llull, Enginyeria I Arquitectura La Salle, Barcelona, Spain, Jul. 2008. [Online]. Available: http://www.tesisenxarxa.net/TDX-0721108-150034/.

86. Cataliotti, A., A. Daidone, and G. Tiné', "Power line communication in medium voltage systems: Characterization of MV cables," *IEEE Trans. Power Del.*, Vol. 23, No. 4, 1896–1902, Oct. 2008.

87. Tang, M. and M. Zhai, "Research of transmission parameters of four-conductor cables for power line communication," *Proc. Int. Conf. on Computer Science and Software Engineering*, Vol. 5, 1306–1309, Wuhan, China, Dec. 2008.

88. OPERA1, D5: Pathloss as a function of frequency, distance and network topology for various LV and MV European powerline networks. IST Integrated Project, No. 507667, Apr. 2005. [Online]. Available: http://www.ist-opera.org/opera1/downloads/D5/D5_Pathloss.pdf.

89. Prasad, T. V., S. Srikanth, C. N. Krishnan, and P. V. Ramakrishna, "Wideband characterization of low voltage outdoor powerline communication channels in India," *Proc. IEEE Int. Conf. Power Line Communications and Its Applications*, 359–364, Malmö, Sweden, Apr. 2001.

90. Issa, F., D. Chaffanjon, and A. Pacaud, "Radiated emission associated with power line communications on low voltage buried cable," *Proc. IEEE Int. Conf. Power Line Communications and Its Applications*, 191–196, Malmö, Sweden, Apr. 2001.